Induction of Metastasis by S100P in a Rat Mammary Model and Its Association with Poor Survival of Breast Cancer Patients

Guozheng Wang, Angela Platt-Higgins, Joe Carroll, Suzete de Silva Rudland, John Winstanley, Roger Barraclough, and Philip S. Rudland

Cancer and Polio Research Fund Laboratories, School of Biological Sciences, University of Liverpool, Liverpool, United Kingdom

Abstract

S100P, an EF-hand calcium-binding protein, has been reported to be associated with the progression of many types of cancers. Transfection of an expression vector for S100P into a benign, nonmetastatic rat mammary cell line causes a 4- to 6-fold increase in its level in all four transformant cell clones. When the resultant transformant cell lines are introduced in turn into the mammary fat pads of syngeneic Furth-Wistar rats, there is a significant 3-fold increase in local muscle invasion and a significant induction of metastasis in 64% to 75% of tumor-bearing animals. In a group of 303 breast cancer patients followed for up to 20 years, antibodies to S100P immunocytochemically stain 161 primary tumors. Survival of patients with S100P-positive carcinomas is significantly worse by about 7-fold than for those with negatively stained carcinomas. There is also a significant association between the class level of immunocytochemical staining of the carcinoma cells and decreased patient survival. Positive staining for S100P is significantly associated with that for two other metastasis-inducing proteins, S100A4 and osteopontin. Patients with tumors that stained positively for both S100P and S100A4 have a significantly reduced survival of 1.1% over patients with either S100 protein alone. Multivariate regression analysis identifies S100P, S100A4, and osteopontin as the most significant independent indicators of death in this group of patients. These results suggest that stratification of patients into groups according to expression of multiple metastasis-inducing proteins may lead to a more accurate prediction of patient survival. (Cancer Res 2006; 66(2): 1199-207)

Introduction

Members of the S100 family of small regulatory calcium-binding proteins, such as S100A2, S100A4, S100A6, S100A7, S100B, and S100P (1–3), have been reported to be associated with many different types of cancers (4). The best studied, S100A4, has been shown to induce metastasis in rodent mammary model systems for breast cancer and to be associated with poor patient outcomes in breast, colon, non–small-cell lung cancer, and esophageal squamous carcinoma (1–4). It is thought to act primarily by binding to the cytoskeleton and altering cellular motility, although extracellular mechanisms have also been suggested (1–4). The gene for another S100 protein, S100P (5), has recently attracted much attention, because it seems to be a differentially expressed gene in many systematic screenings for genes that are up-regulated in malignant tumors compared with their benign counterparts. For example, the gene for S100P is up-regulated in pancreatic cancers (6–9), lung cancer (10), oral squamous cell carcinoma (11), prostatic (12), and breast cancer (13, 14). These observations show a strong association between tumor progression and the elevated expression of S100P. However, it is not clear if the presence of S100P is a causative factor or merely a passenger change in this process. In this study, the metastasis-inducing property of S100P has been investigated in a syngeneic rat model of breast cancer and the association of the presence of S100P in specimens of primary breast carcinomas with the survival of a group of 303 patients with up to 20 years follow-up has been examined using immunocytochemical staining.

Materials and Methods

Plasmid preparation and expression. The S100P coding sequence was amplified from human S100P cDNA by PCR using the following primers: forward 5′-GACAAGCTTATGACGGAACTAGAGACAG and reverse 5′-GGCGGATCCTCATTTGAGTCCTGCCTTCTC. The PCR fragment was digested with *Hind*III and *Bam*HI and subcloned into pCDNA3.1 vector (Invitrogen, Paisley, Scotland) to generate an expression construct, pCDNA-S100P. The identity of the coding sequence for S100P in the pCDNA vector was confirmed by DNA sequencing. Recombinant human S100P (rhS100P) was prepared as previously described (15).

Cell culture and transfection. Rat mammary (Rama) 37, a non-metastatic benign rat mammary tumor-derived cell line (16), expressing undetectable levels of S100P mRNA by Northern and Western blotting, was transfected with pCDNA-S100P or empty pCDNA3.1 as previously described (17). Surviving single-cell colonies were cloned (16) and then grown under selective conditions for 14 days. Two clones expressing high levels of S100P were designated as R37-S100P-1 and R37-S100P-2, whereas the pooled clones, Pool 1 and Pool 2, from two individual transfections were established. Pooled clones from the transfection of pCDNA3.1 expression vector into Rama 37 cells were termed R37 vector.

Northern hybridization. Total RNA was extracted from the single-cell and pooled transfectant cell lines using the guanidinium isothiocyanate-cesium chloride method (18). The separation of RNAs by electrophoresis, blotting, and hybridizations to [^{32}P]dCTP-labeled S100P and β-actin cDNAs were carried out as previously described (17, 19). The bands were quantified using Quantity One software in a Bio-Rad ChemiDoc analyser (Hemel Hempstead, Hertfordshire, United Kingdom).

Western blotting. Fifty micrograms of cell lysates from cultured cells (17) and fresh-frozen specimens of human breast cancers (20), prepared as previously described, were separated on SDS-PAGE gels and then electrically blotted onto Immobilon P membranes (Millipore, Watford, United Kingdom), which were probed with mouse monoclonal antibody (mAb) type immunoglobulin G1 to human S100P (BD Sciences, Cowley, United Kingdom) diluted 1:50 and with polyclonal antibody to S100A4 (DakoCytomation, Glostrop, Denmark) diluted 1:1,000 (17, 21). In some experiments, 100 μg/mL rhS100P or rhS100A4 was preincubated with the mAb to human S100P for 2 hours at room temperature as a blocked antibody control. The bands were visualized using horseradish peroxidase–conjugated secondary antibody and enhanced chemiluminescence (Pierce Biotechnology, Inc., Perbio Science, Framligton, Northumberland, United

Requests for reprints: Philip S. Rudland, School of Biological Sciences, Bioscience Building, University of Liverpool, Liverpool L69 3BX, United Kingdom. Phone: 44-151-795-4474; Fax: 44-151-795-4406; E-mail: wangg@liv.ac.uk.

doi:10.1158/0008-5472.CAN-05-2605

Kingdom) on an X-ray film and were quantified using Quantity One software in a Bio-Rad ChemiDoc analyser.

Tumorigenicity and metastasis. Metastasis assays of transfectant cells were done by injecting 2×10^6 cultured cells s.c. into the mammary fat pad region of syngeneic female Furth-Wistar rats. The histology of tumors and tissues isolated at autopsy after 2 to 3 months was carried out as previously described (16, 22). At least two sections of each tumor/tissue were examined by two independent observers. Animals containing microscopically visible metastases of malignant cells in the lungs and blocks of striated muscle infiltrated by malignant cells at the periphery of the primary tumors were scored positive for metastasis and invasion, respectively. Immunocytochemical staining for S100A4, myoglobin, and general keratins was as previously described (17, 23) and that for S100P was recorded below. Animals were maintained according to UKCCCR guidelines under UK Home Office Project License no. 40/2395 to Prof. P.S. Rudland.

Patients and specimens. Archival formalin-fixed, paraffin-embedded specimens were obtained from primary tumors of 303 unselected patients who presented with operable breast cancer between 1976 and 1982 to general surgery clinics in the Merseyside Region of the North West of England as previously described (20, 24). Treatment was either modified radical mastectomy (83%) or simple mastectomy with sampling of axillary lymph nodes (17%); no adjuvant therapy was given. The age of the patients ranged between 29 and 92 years (average, 57 years) and all had invasive carcinomas. The mean period of follow-up of patients was 16 years ranging from 14 to 20 years. The distribution of tumor sizes, node status, menopausal status, and histologic grade was as previously described (20, 24). Local Ethics Committee Approval was obtained and the patient data were anonymized.

Immunocytochemistry. Histologic sections of 3- to 4-μm thickness prepared from paraffin-embedded sections were dewaxed and immunocytochemically stained using 1:50 diluted mAb to S100P (BD Sciences) and Envision+ system kit (DakoCytomation) according to the instructions of the supplier. Blocked antibody was prepared by mixing mAb to S100P with 100 μg/mL recombinant glutathione *S*-transferase (GST)-S100P fusion protein or with 100 μg/mL rhS100P. Slides from all 303 of the specimens stained by the mAb to hS100P were analyzed independently by two observers using light microscopy. The percentage of stained carcinoma cells was recorded from two sections of each specimen, 10 fields per section at ×200 magnification. Staining for S100P was evaluated in five classes: negative (−), <1%; borderline (±), 1% to 5%; intermediate (+), 5% to 25%; moderate (++), 25% to 50%; and strong (+++), >50% of the carcinoma cells stained, so as to divide the population into roughly equally sized groups, as previously described for the staining for osteopontin (24). Immunocytochemical staining for S100A4 (20), osteopontin (24), c-ERBB-2, cathepsin D, estrogen receptor α, progesterone receptor, pS2, p53, and c-ERBB-3 (25) was as previously described using a 5% cutoff to differentiate between the negatively and positively staining carcinomas. This cutoff yielded the highest risk factor between the two groups in this particular set of patients as previously described (24). Photographs were recorded on a Reichert Polyvar microscope fitted with a Wratten 44 blue green filter (20).

Statistical methods. The association of S100P with tumor cell invasion and metastasis in the rat model and that of immunocytochemical staining for S100P in human breast cancer specimens with other tumor variables (20) was assessed using Fisher's exact test; two-sided values of probability (*P*) are given (26). The cutoff value between those groups of patients designated negatively or positively immunocytochemically stained for the marker proteins was usually set at 5% unless otherwise specified (20, 24, 27, 28). The association of staining for S100P in breast cancers with patient survival was evaluated using life tables constructed from survival

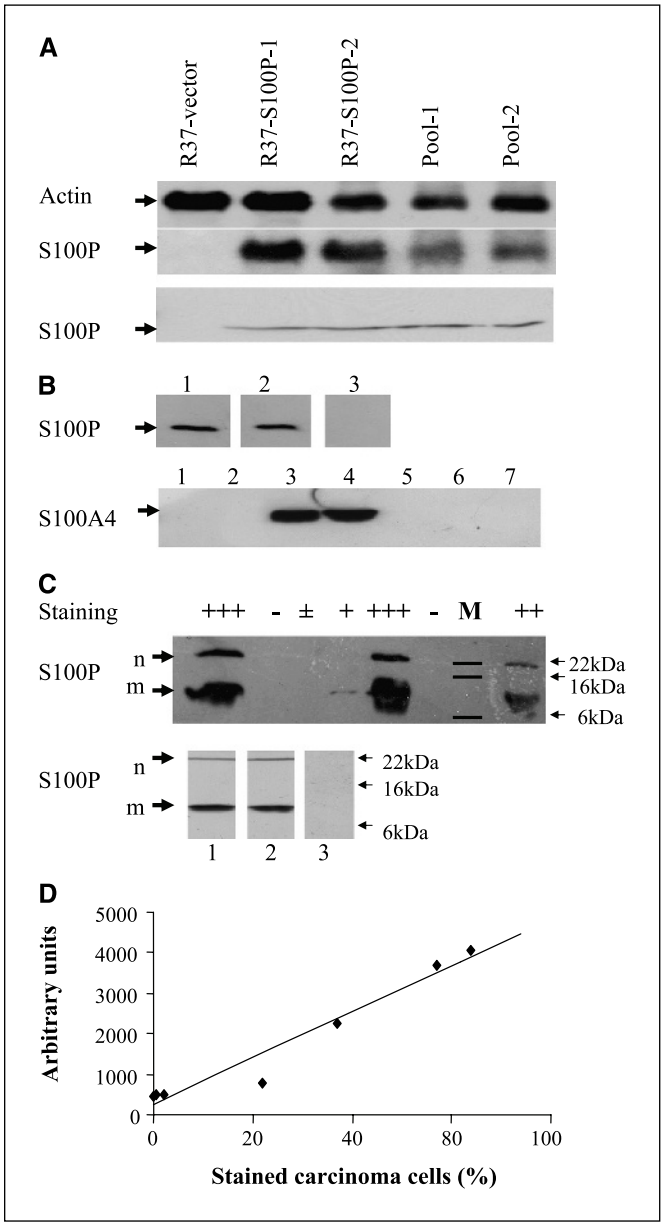

Figure 1. Detection of S100P by Northern and Western blotting. *A, top* and *middle,* Northern blotting. Ten micrograms of total RNA extracted from each cell line were separated by agarose gel electrophoresis and transferred onto a nylon membrane. *Top,* the membrane was hybridized to an actin cDNA and, after stripping, to S100P cDNA (*middle*). *Bottom,* Western blotting. Fifty micrograms of total protein were separated by SDS-PAGE and transferred onto an Immobilon P membrane, which was then incubated with mAb to S100P. *B, top,* 50 μg of lysate from the R37-S100P-1 cell line were loaded in each lane of the SDS-PAGE gel. After electrophoresis, the proteins were then blotted onto an Immobilon P membrane. The membrane was sliced into three pieces, which were separately incubated with mAb to S100P (*lane 1*) or the mAb preincubated with rhS100A4 (*lane 2*) or with rhS100P (*lane 3*). *Bottom,* Western blotting. Fifty micrograms of total protein from each cell lysate, Pool-1 (*lane 1*), Pool-2 (*lane 2*), R37-S100A4 (positive control; *lane 3*), MDA-MB 231 (positive control; *lane 4*), R37-vector (*lane 5*), R37-S100P-1 (*lane 6*), and R37-S100P-2 (*lane 7*) were separated by SDS-PAGE and then transferred onto an Immobilon P membrane, which was then incubated with polyclonal antibody to S100A4. *C, top,* Western blotting. Fifty micrograms of proteins from breast cancer specimens were separated by SDS-PAGE and transferred onto Immobilon P membrane, which was incubated with mAb to S100P. The immunocytochemical staining scores (− to +++) are shown for each sample. *m,* S100P monomer; *n*, S100P polymer. *M,* molecular weight markers shown on the right. *Bottom,* 30 μg of the sample from a human breast cancer specimen (*top, lane 8*) were separated by SDS-PAGE and transferred onto an Immobilon P membrane, which was then sliced and probed as that in (*B, top*). The sliced membranes were incubated with mAb to S100P (*lane 1*) or the mAb preincubated with rhS100A4 (*lane 2*) or the mAb preincubated with rhS100P (*lane 3*). *D,* correlation of the amount of S100P detected by Western blotting [arbitrary units from (*C, top*)] with the percentage of stained carcinoma cells in the corresponding human breast cancer specimen. Least squares regression analysis of the fitting of the points to a straight line yielded $r^2 = 0.96$, $P < 0.01$.

Table 1. Incidence of tumors, muscle invasion, and metastasis by transfected cell lines

Cell lines	S100P	Tumor incidence, *n* (%)*	Invasion of muscle, *n* (%)†	Incidence of metastasis, *n* (%)‡
R37-vector	−	27 of 38 (71)	5 of 18 (28)	0 of 27 (0)
R37-S100P-1	+	18 of 25 (72)	7 of 10 (70)	13 of 18 (72)
R37-S100P-2	+	20 of 25 (80)	13 of 15 (87)	14 of 20 (70)
Pool 1	+	14 of 22 (64)	5 of 7 (71)	9 of 14 (64)
Pool 2	+	8 of 12 (67)	4 of 5 (80)	6 of 8 (75)

*Number of tumors/number of animals inoculated. Tumor incidence of the S100P transfected cells was not significantly different from that of the R37-vector cells (Fisher's exact test, $P \geq 0.21$).
†Numbers of animals with muscle invasion/numbers of animals with tumors adjacent to muscle. Animals that contained no visible muscle blocks were eliminated from the analysis. No significant differences were found in the incidence of muscle invasion among two R37-S100P clones and two Pools ($P \geq 0.31$) of transfectants, but the incidences of these four cell lines were significantly higher than that of R37-vector cells ($P \leq 0.045$).
‡Number of animals with lung metastases/number of animals with tumors. There were no significant differences in the incidence of metastasis among the two separate clones of R37-S100P and two Pools ($P \geq 0.60$), but the incidences of metastasis of R37-S100P-1/-2 or Pool 1/2 were significantly higher than that of R37-vector cells ($P \leq 0.01$).

data with Kaplan-Meier plots and analyzed using generalized Wilcoxon (Gehan) statistics (26). Those patients who died of causes other than cancer were treated as censored observations (27). To assess unadjusted relative risk (RR) for survival and 95% confidence interval (95% CI), a Cox univariate analysis was done as before (26). To determine whether the association of patient survival with S100P was independent of other prognostic factors, a multivariate analysis was done using Cox's proportional hazards model on 136 patients with full data sets (29). Data processing and statistical analyses were done using Excel version 97 (Microsoft Corp., Redmond, WA) and Statistical Package for the Social Sciences version 10.0 (SPSS, Inc., Chicago, IL).

Results

Generation of S100P-overexpressing rat mammary cell lines. The parental Rama 37 cells used for transfection and R37-vector alone cells contained virtually undetectable levels of mRNA and protein for S100P using Northern and Western blotting, respectively (Fig. 1*A*). The Rama 37 cells transfected with the expression vector pCDNA-S100P (R37-S100P-1, R37-S100P-2, Pool 1, and Pool 2) produced an average (±SD) of 10 ± 3.4-fold higher levels of S100P mRNA (0.6 kbp) and 5 ± 1.2-fold higher levels of the S100P protein (10 kDa) than that of R37 vector control (Fig. 1*A*). No S100A4 mRNA or protein was detected in the R37-vector– or pCDNA-S100P–transfected cell lines (Fig. 1*B*). In controls, prior incubation of the mAb with rhS100P, but not with rhS100A4, completely abolished the 10-kDa band in the Western blots of the transfectants (Fig. 1*B*).

Effect of S100P overexpression on invasive and metastasizing ability in rats. S.c. injection into the mammary fat pad region of female Furth-Wistar rats with the transfected cell lines yielded primary tumors in 64% to 80% of the animals; no statistically significant differences were observed between any of these cell lines (Table 1). All transfected cell lines produced tumors with some degree of invasion of the underlying muscle, but all four cell lines overexpressing S100P produced significantly higher (70-87%) muscle invasive tumors (Fig. 2*A*) than that of the 28% due to R37-vector cells ($P \leq 0.045$, Fisher's exact test; Table 1). The R37-vector cells failed to produce any secondary tumors or microscopic lesions on histologic examinations of tissues at autopsy. In contrast, pCDNA-S100P–transfected cell lines produced significantly more lung metastases (64-75% of rats bearing primary tumors) than the R37-vector cells (0%; $P \leq 0.01$, Fisher's exact test; Table 1). Metastases were also observed, but to a lesser extent, in the axillary lymph nodes draining the primary tumor produced by pCDNA-S100P transfectants.

On histologic examination, some metastases in the lungs were smaller, more diffuse, and surrounded by blood vessels (Fig. 2*B*); others were large cannon ball metastases >5 mm in diameter (Fig. 2*C*). Immunocytochemical staining for S100P confirmed that S100P was overexpressed in those tumors/metastases that were produced by the pCDNA-S100P transfectants (Fig. 2*C* and *D*), but not in the primary tumors/lungs of the rats injected with R37-vector cells (not shown). The mAb to S100P stained both the nuclei and the cytoplasm of the tumor cells (Fig. 2*D*) and this staining was completely abolished by prior incubation of the mAb with rGST-S100P (Fig. 2*E*). The primary tumors and metastases of the pCDNA-S100P transfectants consisted of glandlike and spindle cell components as well as large multinucleated cells, all of which stained for S100P (Fig. 2*F*). There was no immunocytochemical staining of any of these tumor cells for S100A4 (Fig. 2*G*). Immunocytochemical staining for general keratins confirmed the epithelial nature of the glandlike elements in both the primary tumors and metastases (not shown). On inspection of histologic sections, the numbers of peripheral blood vessels adjacent to the invasive edge of the primary tumors were not appreciably different for any of the transfectant cell lines, including the R37-vector cells, nor were these vessels stained for S100P although large numbers of infiltrating lymphocytes were stained intensely (Fig. 2*H*).

Immunocytochemical staining of human breast carcinomas for S100P. Immunocytochemical staining of normal human parenchymal breast tissues was, with the exception of ductal hyperplasias and carcinoma *in situ*, relatively unstained (not shown), whereas that of breast carcinomas ranged from none (Fig. 3*A*) to >90% of carcinoma cells staining (Fig. 3*B* and *C*). Of the 303 invasive breast carcinomas evaluated, 62 (20.5%) were classified as unstained (−; <1% of carcinoma cells stained; Fig. 3*A*); 80 (26.4%) were borderline stained (±; 1-5% carcinoma cells stained; Fig. 3*B*), and the remaining 161 (53.1%) were stained to some degree by the mAb to S100P. These were further subdivided into classes of 60 (19.8%) moderate (+; 5-25% cells stained), 53 (17.5%) strong (++; 25-50% cells stained), and 48 (15.8%) very strong (>50% of

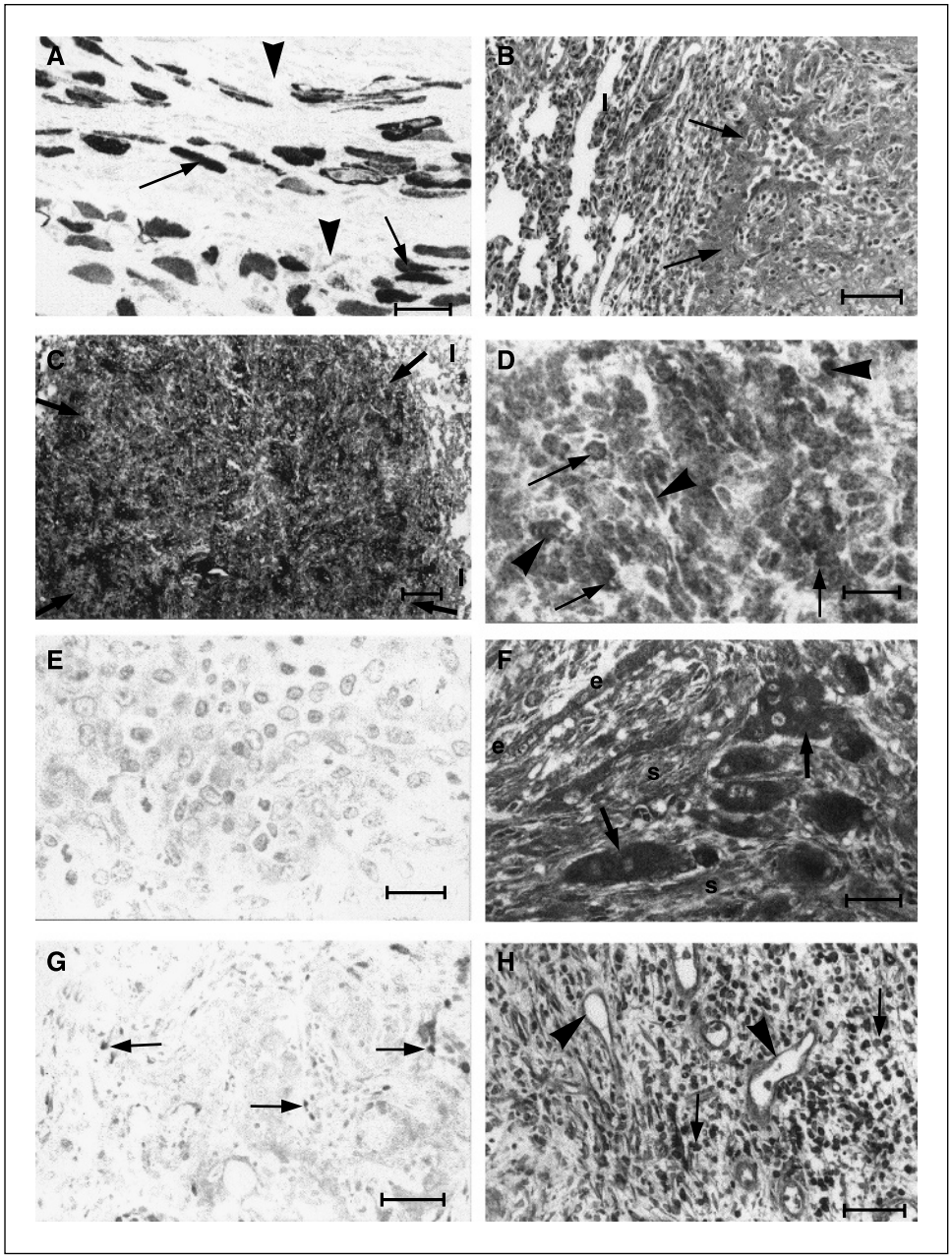

Figure 2. Immunocytochemical staining of tumors and metastases produced by S100P in rats. *A,* primary tumor produced by R37-S100P-1 cells incubated with antimyoglobin showing cells (*arrowheads*) invading underlying stained muscle (*arrow*). *B,* lung metastasis produced by R37-S100P-1 cells stained with H&E showing glandlike epithelial cells (*arrows*) permeating the lung (*l*). *C,* lung metastasis produced by R37-S100P-1 cells incubated with anti-S100P showing a large stained cannon ball metastasis (*arrows*); the remainder of the lung (*l*) is unstained. *D,* lung metastasis produced by R37-S100P-1 cells incubated with anti-S100P showing at higher power staining of the nucleus (*arrowheads*) and cytoplasm (*arrows*) of the glandlike tumor cells. *E,* serial section to (*D*) incubated with anti-S100P blocked by prior incubation with rGST-hS100P showing no staining. *F,* primary tumor produced by R37-S100P-2 cells incubated with anti-S100P showing staining of large multinucleated cells (*arrows*) in addition to epithelial-like (*e*) and spindle cells (*s*). *G,* lung metastasis produced by R37-S100P-2 cells incubated with anti-S100A4 showing no staining of the tumor cells but with staining of the occasional lymphocyte (*arrows*). *H,* invasive edge of primary tumor produced by R37-S100P-2 cells incubated with mAb to S100P showing intense staining of lymphocytes (*arrows*) but no staining of blood vessels (*arrowheads*). Magnification: ×230 (*A, B, F, G*, and *H*); ×72 (*C*); and ×580 (*D* and *E*). Bar: 50 μm (*A, B, F, G*, and *H*); 100 μm (*C*); and 20 μm (*D* and *E*).

carcinoma cells stained) staining carcinomas (Fig. 3*C*). For most analyses, the borderline staining carcinomas were combined with the unstained carcinomas into one group of negatively stained carcinomas, leaving the clearly positive staining carcinomas as the other categorical group. There was a good degree of consistency between the two observers with agreement in 94.8% of cases corresponding to a κ score of 0.92. Intratumor heterogeneity was higher than this at 6.9% for two well-separated sections of the same tumor. In the latter cases, additional sections were immunocytochemically stained and analyzed to obtain a consensus result.

The immunochemical staining for S100P was predominantly nuclear with some cytoplasmic staining (Fig. 3*C*) and was abolished by prior incubation of the mAb with rGST-S100P (Fig. 3*D*). In positive staining carcinomas, the mAb failed to stain the majority of blood vessels adjacent to the invasive edge of the tumor (Fig. 3*E*). However, when this mAb was preincubated with rhS100P lacking the GST fusion protein, staining of the cytoplasm, membrane, and extracellular matrix of the carcinoma cells and that of the same peripheral blood vessels dramatically increased (Fig. 3*F*). This was particularly evident at higher microscopic power (Fig. 3*G* and *H*). Preincubation of the mAb to S100P with rhS100A1 produced no such change (not shown).

When tested in Western blots of extracts from immunocytochemically positive breast carcinomas, the mAb to S100P detected two bands: a major of 10 kDa and a minor of 20 kDa apparent molecular weight (Fig. 1*C*), which corresponded in size to that of monomers and dimers of authentic rhS100P (Fig. 1*C*). Their appearance was abolished by prior incubation of the mAb with rhS100P (Fig. 1*C*) but not with rhS100A4 (not shown). The appearance of the dimer may be due to the preparation procedures of the human sample (20). In seven samples chosen at random, there was a significant correlation between the level of immunodetectable

S100P by Western blotting and the percentage of cells immunocytochemically stained for S100P ($r^2 = 0.96$, $P = 0.01$; Fig. 1*D*).

Association of S100P with other tumor variables. The presence of definitely positive immunocytochemical staining for S100P was cross-tabulated with other tumor variables associated with outcome in this group of patients (20, 24); these included tumor size, histologic grade, nodal status, and the immunocytochemical presence of S100A4, osteopontin, c-ERBB-2, c-ERBB-3, cathepsin D, p53, estrogen receptor α, progesterone receptor, and pS2 (Table 2). The cutoff levels of all tumor variables were set at 5% of the carcinoma cells stained and statistical significance was assessed using Fisher's exact test. A significant association of staining for S100P was observed with five of the prognostic markers including S100A4 ($P < 0.0001$), osteopontin ($P < 0.0001$), c-ERBB-3 ($P < 0.0001$), cathepsin D ($P = 0.001$), and pS2 ($P = 0.026$). Carcinomas in the axillary lymph nodes showed a borderline association with immunocytochemical staining for S100P in the primary tumor ($P = 0.060$; Table 2). If the cutoff levels were set at 1% for S100P and 5% for the other immunocytochemically detected tumor variables, a significant association of staining for S100P was found with that for S100A4 ($P < 0.0001$), osteopontin ($P < 0.0001$), c-ERBB-3 ($P = 0.031$), p53 ($P = 0.028$)l, and carcinoma in axillary lymph nodes ($P = 0.012$; data not shown).

Association of S100P and patient survival. The association of immunocytochemical staining for S100P and the cumulative proportion of patients surviving at yearly intervals after the time of presentation are shown in Fig. 4. Patients were divided into two classes using a 5% cutoff: S100P(−) with <5% carcinoma cells stained and S100P(+) with >5% carcinoma cells stained. Of the 142 patients who were classified as S100P(−), 82.5% were alive at the census date with a median survival time of >216 months, in comparison with 16.9% of the 161 patients classified as S100P(+)

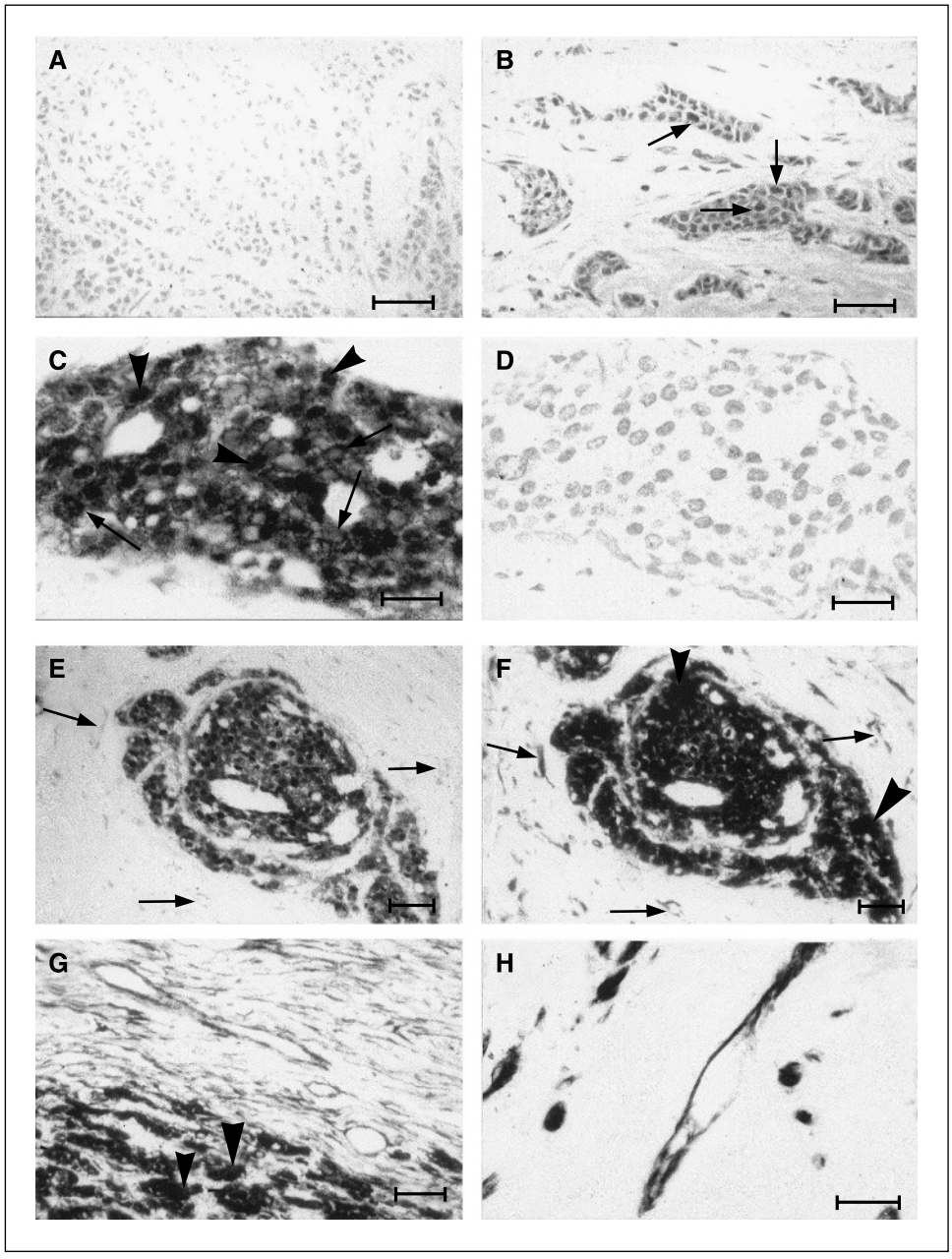

Figure 3. Immunocytochemical staining of human breast carcinomas for S100P. *A,* invasive carcinoma showing no staining for S100P. *B,* invasive carcinoma showing borderline staining (±) of 3% to 5% carcinoma cells stained for S100P (*arrows*). *C,* invasive carcinoma showing at high power very strong staining (+++) of >70% carcinoma cells stained for S100P; the majority of the stain was nuclear (*arrowheads*) with some cytoplasmic staining (*arrows*). *D,* serial adjacent section to (*C*) incubated with mAb to S100P preincubated with GST-hS100P showing no staining. *E,* invasive carcinoma at lower power showing predominantly nuclear staining for S100P; virtually no vessels adjacent to the invasive edge of the tumor were stained (*arrows*). *F,* serial adjacent section to (*E*) incubated with mAb to S100P preincubated with rhS100P showing an increase in cytoplasmic (*arrowheads*) and matrix staining, particularly that of vessels adjacent to the invasive edge of the tumor (*arrows*), over that in (*E*). *G* and *H,* sections incubated with mAb preincubated with rhS100P shown at higher power. *G,* strongly stained cytoplasm and extracellular matrix; *H,* strongly stained endothelial cells lining a blood vessel. Magnification: ×230 (*A* and *B*); ×580 (*C, D*, and *H*); and ×185 (*E-G*). Bar: 50 μm (*A, B, E, F*, and *G*); and 20 μm (*C, D*, and *H*).

Table 2. Association of staining for S100P with other tumor variables

Tumor variables*	S100P negative, n † (%)	S100P positive, n † (%)	P ‡
Lymph node−	64 (59.3)	53 (46.1)	0.060
Lymph node+	44 (40.7)	62 (53.9)	
Grade 1, 2	96 (78.7)	109 (74.1)	0.39
Grade 3	26 (21.3)	38 (25.9)	
Tumor size 1, 2	103 (75.7)	119 (76.3)	1.00
Tumor size 3, 4	33 (24.3)	37 (23.7)	
Osteopontin−	85 (59.9)	20 (12.9)	<0.0001
Osteopontin+	57 (40.1)	135 (87.1)	
Estrogen receptor α−	67 (46.9)	78 (50)	0.64
Estrogen receptor α+	76 (53.1)	78 (50)	
C-ERBB-2−	78 (54.9)	44 (28.4)	<0.0001
C-ERBB-2+	64 (45.1)	111 (71.6)	
C-ERBB-3−	78 (54.9)	44 (28.4)	<0.0001
C-ERBB-3+	64 (45.1)	111 (71.6)	
S100A4−	125 (85)	64 (40)	<0.0001
S100A4+	22 (15)	96 (60)	
Progesterone receptor−	92 (66.2)	87 (56.9)	0.12
Progesterone receptor+	47 (33.8)	66 (43.1)	
p53−	98 (67.1)	92 (57.9)	0.100
p53+	48 (32.9)	67 (42.1)	
Cathepsin D−	59 (53.2)	38 (30.4)	0.001
Cathepsin D+	52 (46.8)	87 (69.6)	
pS2−	97 (66.4)	84 (53.5)	0.026
pS2+	49 (33.6)	73 (46.5)	

*Lymph node with tumor (+) or without tumor (−); grade, histologic grade 3 versus histologic grades 1, 2; tumor sizes >5 cm or fixed to the chest wall (sizes 3,4) versus tumor <5 cm in diameter (sizes 1, 2); for the rest of the tumor variables, the presence (+) or absence (−) of immunocytochemical staining using a cutoff of 5% of the carcinoma cells stained.

†Number of patients with carcinomas either classified as staining (+, positive) or not staining (−, negative) for S100P. Parentheses show the percentage of patients.

‡Probability between paired samples from Fisher's exact test (two-sided value).

with a median survival time of 59.4 months. Over the full follow-up period of 20 years, the survival of patients with S100P-positive carcinomas was highly significantly worse than those patients with carcinomas classified as S100P-negative (Wilcoxon test, $P < 0.0001$) with RR of increased death from cancer of 7.3 (95% CI, 4.7-11.5; Fig. 4*A*). These differences became significant after 2 years of follow-up. If the cutoff levels were set at 1% instead of 5% of the carcinoma cells staining for S100P, the two groups of patients were still highly significantly different (Wilcoxon test, $P < 0.0001$) with RR of 27 (95% CI, 6.7-109).

When the patients were divided into their separate classes based on the percentage of carcinoma cells staining for S100P and analyzed separately for their outcome, there was a highly significant association of the class level of staining for S100P and decreased patient survival (Wilcoxon test, $P < 0.0001$; Fig. 4*B*). These differences become significant after 1 year. The negative (−), borderline (±), and moderate (+) staining classes showed a significant progressive decrease in patient survival of 96.5%, 71.9%, and 24.8%, respectively, corresponding to median survival times of >216, >216, and 57 months (Wicoxon test, $P \leq 0.0002$), whereas there was no significant difference in survival between those patients with different classes of positively staining tumors ($P \geq 0.67$; Fig. 4*B*). These progressive decreases in survival corresponded to progressive increases in RR of demise from breast cancer between the negative (−)/borderline (±), the borderline (±)/moderate (+), and the moderate (+)/strong (++) staining groups of 10.3 (95% CI, 2.4-44), 3.6 (95% CI, 2.1-6.1), and 1.3 (95% CI, 0.8-2.1) respectively, yielding an overall difference in RR of 47 (95% CI, 11-200) between the negative (−) and strong (++) or very strong (+++) staining groups.

Association of S100P and other tumor variables with patient survival. To investigate how S100P associates with the metastasis-inducing S100A4 (22) to influence patient survival, the patients were subdivided into four subgroups based on a cutoff of 5% carcinoma cells staining for S100P and S100A4; those below this cutoff were designated (−) and those above (+). Patients with unstained tumors [S100P(−)/S100A4(−)] had a survival of 90.5% and a median survival time of >216 months. Patients with tumors positively stained for only one S100 protein [S100P(+)/S100A4(−) or S100P(−)/S100A4(+)] had a significantly reduced survival of 48.2% (median 173 months) or 40.2% (median 72 months), respectively, over the completely unstained group (Wilcoxon statistics $\chi^2 = 20.5$ or 29.5, $P < 0.0001$). The RRs were 6.3 (95% CI, 3.1-12.9) or 9.8 (95% CI, 4.4-22), respectively. However, there was only a difference of borderline significance between these two groups of patients [$\chi^2 = 2.9$, 1 degree of freedom (*df*), $P = 0.088$] with RR of 1.6 (95% CI, 0.8-3.1). The patients with tumors stained for both S100 proteins had a significantly reduced survival of only 1.1% (median 42 months) over the patients with either S100P(+)/S100A4(−) ($\chi^2 = 34.9$, 1 *df*, $P < 0.0001$) or S100P(−)/S100A4(+) ($\chi^2 = 7.4$, 1 *df*, $P = 0.0065$) tumors. The RR was 4.0 (95% CI, 2.6-6.4) or 2.6 (95% CI, 1.5-4.7), respectively.

To determine whether the tumor variables that showed a significant association with outcome in this group of patients (20, 24) were independent of one another, all 13 were included in a multivariate regression analysis for the 136 patients available with full data sets using 5% cutoff staining levels where appropriate (Materials and Methods). The first variable to emerge and most significant of all was staining for S100A4 (Cox test $\chi^2 = 14.5$, 1 *df*, $P < 0.001$) followed by that for osteopontin ($\chi^2 = 9.5$, 1 *df*, $P = 0.002$), involved lymph nodes ($\chi^2 = 6.2$, 1 *df*, $P = 0.013$), S100P ($\chi^2 = 5.9$, 1 *df*, $P = 0.015$), and estrogen receptor α ($\chi^2 = 4.8$, 1 *df*, $P = 0.029$). On controlling the data for S100A4, osteopontin, involved lymph nodes, S100P, and estrogen receptor α (overall $\chi^2 = 81.9$, 5 *df*, $P < 0.001$), there was no significant independent association between large tumor size, high histologic grade, staining for c-ERBB-2, c-ERBB-3, cathepsin D, p53, progesterone receptor, pS2, and patient survival (Cox analysis, residual $P = 0.08$). The adjusted RR for death of women with S100P-positive carcinomas was 2.1 (95% CI, 1.2-3.9) compared with that for S100A4, osteopontin, involved lymph nodes, and estrogen receptor α of 3.2 (95% CI, 1.8-5.7), 5.3 (95% CI, 1.8-15), 1.9 (95% CI, 1.1-3.0), and 0.58 (95% CI, 0.36-0.95), respectively. When both staining for S100A4 and osteopontin were omitted from the data sets (144 patients), the first two tumor variables to emerge and the most significant was staining for S100P ($\chi^2 = 28.9$, 1 *df*, $P < 0.001$) with a RR of 4.7(95% CI, 2.7-8.3), followed by c-ERBB-2 ($\chi^2 = 10.33$, 1 *df*, $P = 0.001$) with a RR of 2.3 (95% CI, 1.4-3.7); staining for estrogen receptor α was of borderline significance ($P = 0.088$; overall $\chi^2 = 43.3$, 2 *df*, $P < 0.001$). The remainder of the tumor variables were not significantly independently associated

with patient survival (residual χ^2 = 11.4, 9 *df*, P = 0.25). As soon as S100P emerged in the first step of the analysis, the independent significance of association of tumor involved lymph nodes with patient survival was lost (χ^2 = 1.83, 1 *df*, P = 0.18).

Discussion

Transfection of S100P cDNA in an expression vector into the benign rat mammary cell line, Rama 37, produces a protein consistent with the size of S100P (5) in two independent single-cell clones and two clone pools. All four transfectants induce metastases *in vivo* whereas similar transfectant with the vector alone failed to induce any metastases as before (17, 30–32). The use of pooled clones and two single-cell cloned cell lines overexpressing S100P eliminates the possibility of spontaneous induction of metastasis in the benign Rama 37 cell line (33). The fact that the primary tumors and lung/lymph node metastases produced by the four S100P cDNA transfectants possess the same histology, including the giant polynucleated cells, and can be immunocytochemically stained for S100P, whereas the primary tumors produced by the vector-alone transfectants are not, strongly suggests that the metastases develop as a result of the expression of S100P. Moreover, overexpression of the closely related metastasis-inducing S100A4 (22) is not detected in the S100P cDNA transfectants, either in culture or in metastatic lesions *in vivo*, thus eliminating the possibility that the metastases are due to the presence of endogenous S100A4. Although S100P has been shown to occur preferentially in malignant as opposed to nonmalignant disease (13, 34), particularly that of the pancreas (6, 7), this is the first formal demonstration that S100P can directly induce metastasis *in vivo*. The appearance of the lung metastases as diffuse, often surrounding blood vessels and as cannon balls is consistent with lymphatic and blood borne spread, respectively (35).

The potential clinical relevance of the overexpression of S100P has been sought using immunocytochemistry on primary tumors of a group of 303 breast cancer patients with follow-up of up to 20 years. In agreement with others, there is little staining of normal glandular tissue (6, 7, 13). There is, however, a heterogeneous staining pattern for the primary tumor, consistent with that observed in other studies with very much smaller numbers of patients (6, 13). When the tumor variables which show a significant association with outcome in this group of breast cancer patients are tested for association with immunocytochemical staining for S100P in the primary carcinomas, staining for the metastasis-inducing proteins S100A4 (22) and osteopontin (30) is the most significantly associated at both the 5% and 1% cutoff levels for staining for S100P. These results may suggest that the same

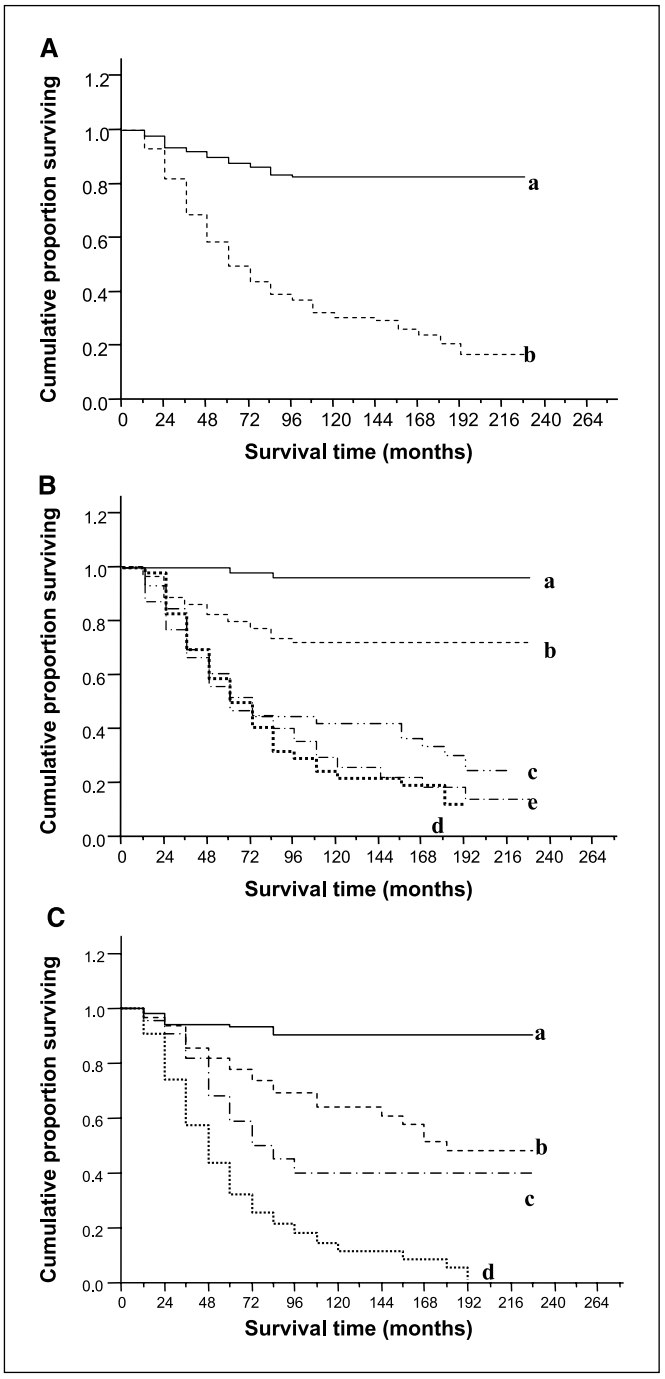

Figure 4. Association of immunocytochemical staining for S100P with overall survival of patients. *A,* the cumulative proportion of surviving patients as a fraction of the total for each year after presentation for patients with carcinomas classified either as negatively staining using a cutoff of 5% (—; *a*) or positively staining (- - -; *b*) for S100P. For S100P-negative carcinomas, 100% corresponds to 142 and, for S100P-positive carcinomas, to 161 patients. There were 118 censored observations in *a* (22 dead of other causes) and 48 in *b* (32 dead of other causes). The two curves are highly significantly different (Wilcoxon statistics χ^2 = 73.3, 1 *df*, P < 0.0001). *B,* the cumulative proportion of surviving patients as a fraction of the total classified as follows: −, completely negative staining (—; 100% = 62 patients; *a*); ±, borderline staining (- - -; 100% = 80 patients; *b*); +, moderate staining (– · · –; 100% = 60 patients; *c*); ++, strong staining (■■■■; 100% = 53 patients; *d*); and +++, very strong staining (– · – · –; 100% = 48 patients; *e*) for S100P. There were 60 censored observations in *a* (10 dead of other causes); 58 in *b* (12 dead of other causes); 23 in *c* (14 dead of other causes); 13 in *d* (10 dead of other causes); and 12 in *e* (8 dead of other causes). The curves are highly significantly different (Wilcoxon statistics χ^2 = 82.72, 4 *df*, P < 0.0001) and significantly different in the successive pairwise combinations for *a* with *b* (χ^2 = 14.62, 1 *df*, P = 0.0001) and *b* with *c* (χ^2 = 14.16, 1 *df*, P = 0.0002), but not for *c* with *d* (χ^2 = 0.18, 1 *df*, P = 0.67) nor *d* with *e* (χ^2 = 0.01, 1 *df*, P = 0.91). *C,* the cumulative proportion of surviving patients as a fraction of the total classified as S100P(−)/S100A4(−) staining (—; 100% = 120 patients; *a*); S100P(+)/S100A4(−) staining (- - -;100% = 64; *b*); S100P(−)/S100A4(+) staining (– · – · –;100% = 22 patients; *c*); and S100P(+)/S100A4(+) staining (■■■■; 100% = 96 patients; *d*). There were 109 censored observations in *a* (19 dead of other causes); 40 in *b* (22 dead of other causes); 9 in *c* (3 dead of other causes); and 7 in *d* (5 dead of other causes). The curves are highly significantly different (Wilcoxon statistics χ^2 = 129.7, 3 *df*, P < 0.0001) and significantly different in the successive pairwise combinations for *a* with *b* (χ^2 = 20.5, 1 *df*, P < 0.0001), *b* with *d* (χ^2 = 34.9, 1 *df*, P < 0.0001), and *c* with *d* (χ^2 = 7.4, 1 *df*, P = 0.0065), but not for *b* with *c* (χ^2 = 2.9, 1 *df*, P = 0.088).

underlying change(s) is responsible for the altered expression of these three metastasis-inducing proteins. One other consistent association of S100P with a tumor variable is that with carcinoma in the lymph nodes; this association is of borderline significance at 5% (Fisher exact test, $P = 0.06$) and significant at 1% cutoff levels ($P = 0.012$) of carcinoma cells staining for S100P. Because the nodal status has been recorded for only 74% of the tumors in this study, this smaller number may render the tests for its positive association with S100P less significant than it may otherwise have been.

The overall survival for patients with carcinomas stained positively for S100P is shown to be highly significantly worse than for patients with carcinomas classified as negatively stained (Wilcoxon statistics $\chi^2 = 73.3$, $P < 0.0001$) and comparable to that for the other two metastasis-inducing proteins, S100A4 ($\chi^2 = 131.5$, $P < 0.0001$; ref. 20) and osteopontin ($\chi^2 = 95.4$, $P < 0.0001$; ref. 24), as well as with involved lymph nodes ($\chi^2 = 17.3$, $P < 0.0001$; ref. 20). The RR of death of patients with S100P positive tumors is 7.3 (95% CI, 4.5-11.5) in this group of patients, smaller than that for S100A4 of 8.7 (95% CI, 6.7-12.7; ref. 20) and osteopontin of 21.5 (95% CI, 9.5-48.9; ref. 24), but still considerably higher than that for involved lymph nodes of 2.1 (95% CI, 1.4-3.0; ref. 20). This relationship for S100P achieved statistical significant after 2 years compared with that for S100A4 after 6 months and for osteopontin after 1 year of follow-up. The fact that comparable results are obtained for S100P at the 1% (not shown) as well as the 5% cutoff level means that their significance is not dependent on one arbitrary cutoff level dividing the negative and positively staining groups of tumors. Grouping the patients into classes according to the % carcinoma cells staining for S100P shows that not only the presence but also the proportion of carcinoma cells staining for S100P up to a limit of 25% is correlated with the time of death of the patients. This result suggests that the levels of immunoreactive S100P may be correlated with their time of death. The fact that the presence of immunoreactive S100P is so closely correlated with early death in this group of patients may suggest that this change, like that of S100A4 and osteopontin, is closely associated with its cause, possibly by its ability to induce metastasis in humans.

Although both S100P and S100A4 can independently induce metastasis in the same rat mammary cell system and both are associated with poor outcomes of breast cancer patients, there are some obvious differences. First, immunocytochemical staining of the carcinoma cells in human breast cancers localizes S100P predominantly to the nucleus with a weak staining in the cytoplasm, like S100A2 (36) and S100A6 (37). In contrast, S100A4 (37) occurs predominantly in the cytoplasm and extracellularly, like S100B (38), particularly in endothelial cells in vessels adjacent to stained carcinomatous areas.[1] Moreover, when serial adjacent sections are incubated with rhS100P complexed with mAb to S100P, staining in the cytoplasm and extracellular matrix, particularly that of the endothelial cells, is enhanced in the rat and human tumors (Fig. 3*E-H*). The staining pattern is now similar to that for antibodies to S100A4.[1] However, blocking controls of the mAb to S100P with the fusion protein GST-S100P abolish all staining of histologic sections of S100P-positive tumors (Figs. 2*E* and 3*D*) and this inhibition is not due to simple interference by GST of the binding of the S100P mAb (data not shown). The more likely explanation is that there are potential receptors for S100P in the cytoplasm/extracellular matrix/endothelial cells which are unoccupied and antibody-bound S100P can locate them, as previously described for fibroblast growth factor 2 (39). The GST protein fused at the NH_2 terminus of S100P may disturb a potential binding site on S100P for its binding partners, thereby abolishing staining completely. These conclusions are consistent with an extracellular role for S100A4[1] in stimulating tumor angiogenesis (40, 41), which would seem to be largely absent in the case of S100P in human breast cancer.

When those tumor variables which are associated with patient outcome are assessed in the Cox proportional hazards model, immunocytochemical stainings for all three metastasis-inducing proteins together with involved lymph nodes and estrogen receptor α emerge as significant independent prognostic indicators. The fact that large tumor size, high histologic grade, and staining for c-ERBB-2, c-ERBB-3, p53, progesterone receptor, pS2, and cathepsin D are rejected as independent prognostic factors in the Cox multivariate analysis may suggest that they are confounded by one or more of the independent prognostic variables in the proportional hazards model. When the results for two of the metastasis-inducing proteins are left out in turn, the remaining metastasis-inducing protein emerges as the most significant: S100A4, $P < 0.0001$, RR = 7.5 (20); osteopontin, $P < 0.0001$, RR = 12.9 (24); and S100P, $P < 0.001$, RR = 4.7. As soon as S100P emerges in the first step of the analysis as the most significant tumor variable, the independent significance of the association of tumor-involved lymph nodes is lost. This result is in contrast to that for S100A4 and osteopontin in which involved lymph nodes remain significantly associated with patient survival after the final analysis. These results suggest that of the three metastasis-inducing proteins, the one most closely associated with involved lymph nodes is S100P in relation to patient survival. When all the data are combined, the order the tumor variables emerge is in agreement with the results of subgroups of patients with tumors staining for S100P and/or S100A4 or S100P and/or osteopontin. Moreover, patients with S100A4(+)/S100P(+) tumors (Fig. 4*C*) or osteopontin (+)/S100P(+) tumors (not shown) are likely to die significantly earlier than patients with S100A4(+)/S100P(−) or osteopontin (+)/S100P(−) tumors, the RR being 2.6 (95% CI, 1.4-4.7) and 3.3 (95% CI, 2.1-5.3), respectively. The RR for patients with S100A4(+)/S100P(+) tumors compared with those with S100A4(−)/S100P(−) tumors at 26 (95% CI, 13-49) and the RR for patients with osteopontin (+)/S100P(+) tumors compared with those with osteopontin (−)/S100P(−) tumors at 143 (95% CI, 20-1030) are both extremely high. These results show that the use of multiple metastasis-inducing proteins can pinpoint subgroups of patients that are likely to do well or badly much more accurately than those with either one metastasis-inducing protein alone or with the expression profile of 70 selected genes in array analyses (42). Moreover, in the case of S100P and S100A4, two structurally similar molecules (15, 43), stratification of patients into one group opens the way in the future to target this group with the same medicinal compound active against both metastasis-inducing proteins.

Acknowledgments

Received 7/25/2005; revised 10/20/2005; accepted 10/26/2005.

Grant support: Cancer and Polio Research Fund.

The costs of publication of this article were defrayed in part by the payment of page charges. This article must therefore be hereby marked *advertisement* in accordance with 18 U.S.C. Section 1734 solely to indicate this fact.

We thank C. Holcombe and the Breast Unit, Royal Liverpool University Hospital, for clinical assistance; Dr. E.M.I. Williams and the staff of the Merseyside and Cheshire Cancer Registry for providing patient outcome data; and Barry Cottrell and Karen Collard for excellent technical assistance.

[1] de Silva Rudland et al., Clinical Cancer Research, submitted for publication.

References

1. Donato R. S100: a multigenic family of calcium-modulated proteins of the EF-hand type with intracellular and extracellular functional roles. Int J Biochem Cell Biol 2001;33:637–68.
2. Zimmer DB, Wright Sadosky P, Weber DJ. Molecular mechanisms of S100-target protein interactions. Microsc Res Tech 2003;60:552–9.
3. Heizmann CW, Fritz G, Schäfer BW. S100 proteins: structure, functions and pathology. Front Biosci 2002; 7:D1356–68.
4. Marenholz I, Heizmann CW, Fritz G. S100 proteins in mouse and man: from evolution to function and pathology (including an update of the nomenclature). Biochem Biophys Res Commun 2004;322:1111–22.
5. Becker T, Gerke V, Kube E, Weber K. S100P, a novel Ca^{2+}-binding protein from human placenta. cDNA cloning, recombinant protein expression and Ca^{2+} binding properties. Eur J Biochem 1992;207:541–7.
6. Crnogorac-Jurcevic T, Missiaglia E, Blaveri E, et al. Molecular alterations in pancreatic carcinoma: expression profiling shows that dysregulated expression of S100 genes is highly prevalent. J Pathol 2003;201: 63–74.
7. Logsdon CD, Simeone DM, Binkley C, et al. Molecular profiling of pancreatic adenocarcinoma and chronic pancreatitis identifies multiple genes differentially regulated in pancreatic cancer. Cancer Res 2003;63: 2649–57.
8. Fukushima N, Sato N, Prasad N, Leach SD, Hruban RH, Goggins M. Characterization of gene expression in mucinous cystic neoplasms of the pancreas using oligonucleotide microarrays. Oncogene 2004;23:9042–51.
9. Missiaglia E, Blaveri E, Terris B, et al. Analysis of gene expression in cancer cell lines identifies candidate markers for pancreatic tumorigenesis and metastasis. Int J Cancer 2004;112:100–12.
10. Diederichs S, Bulk E, Steffen B, et al. S100 family members and trypsinogens are predictors of distant metastasis and survival in early-stage non-small cell lung cancer. Cancer Res 2004;64:5564–9.
11. Li Y, St. John MA, Zhou X, et al. Salivary transcriptome diagnostics for oral cancer detection. Clin Cancer Res 2004;10:8442–50.
12. Mousses S, Bubendorf L, Wagner U, et al. Clinical validation of candidate genes associated with prostate cancer progression in the CWR22 model system using tissue microarrays. Cancer Res 2002;62:1256–60.
13. da Silva IDG, Hu YF, Russo IH, et al. S100P calcium-binding protein overexpression is associated with immortalization of human breast epithelial cells *in vitro* and early stages of breast cancer development *in vivo*. Int J Oncol 2000;16:231–40.
14. Mackay A, Jones C, Dexter T, et al. cDNA microarray analysis of genes associated with ERBB2 (HER2/neu) overexpression in human mammary luminal epithelial cells. Oncogene 2003;22:2680–8.
15. Zhang H, Wang G, Ding Y, et al. The crystal structure at 2Å resolution of the Ca^{2+}-binding protein S100P. J Mol Biol 2003;325:785–94.
16. Dunnington DJ, Hughes CM, Monaghan P, Rudland PS. Phenotypic instability of rat mammary tumor epithelial cells. J Natl Cancer Inst 1983;71:1227–40.
17. Wang G, Zhang S, Fernig DG, Martin-Fernandez M, Rudland PS, Barraclough R. Mutually antagonistic actions of S100A4 and S100A1 on normal and metastatic phenotypes. Oncogene 2005;24:1445–54.
18. Barraclough R, Kimbell R, Rudland PS. Differential control of mRNA levels for Thy-1 antigen and laminin in rat mammary epithelial and myoepithelial-like cells. J Cell Physiol 1987;131:393–401.
19. Sambrook J, Fritsch EF, Maniatis T. 2nd ed. In: Molecular Cloning: A Laboratory Manual. New York (NY): Cold Spring Harbor Laboratory Press, Cold Spring Harbor; 1989.
20. Rudland PS, Platt-Higgins A, Renshaw C, et al. Prognostic significance of the metastasis-inducing protein S100A4 (p9Ka) in human breast cancer. Cancer Res 2000;60:1595–603.
21. Wang G, Zhang Z, Fernig DG, et al. Heterodimerisation and the heterodimeric interfaces of S100A1 and S100P. Biochem J 2004;382:375–83.
22. Davies BR, Davies MP, Gibbs FEM, Barraclough R, Rudland PS. Induction of the metastatic phenotype by transfection of a benign rat mammary epithelial cell line with the gene for p9Ka, a rat calcium-binding protein, but not with the oncogene EJ-ras-1. Oncogene 1993;8: 999–1008.
23. Jenkinson SR, Barraclough R, West CR, Rudland PS. S100A4 regulates cell motility and invasion in an *in vitro* model for breast cancer metastasis. Br J Cancer 2004;90: 253–62.
24. Rudland PS, Platt-Higgins A, El-Tanani M, et al. Prognostic significance of the metastasis-associated protein osteopontin in human breast cancer. Cancer Res 2002;62:3417–27.
25. Platt-Higgins AM, Renshaw CA, West CR, et al. Comparison of the metastasis-inducing protein S100A4 (p9ka) with other prognostic markers in human breast cancer. Int J Cancer 2000;89:198–208.
26. Altman DG. Practical Statistics for Medical Research. London: Chapman and Hall; 1991. p. 403–5.
27. Winstanley J, Cooke T, Murray GD, et al. The long term prognostic significance of c-erbB-2 in primary breast cancer. Br J Cancer 1991;63:447–50.
28. Winstanley JH, Leinster SJ, Cooke TG, Westley BR, Platt-Higgins AM, Rudland PS. Prognostic significance of cathepsin-D in patients with breast cancer. Br J Cancer 1993;67:767–72.
29. Cox DR. Regression models and life tables. J Roy Stat Soc B (Lond) 1972;34:187–202.
30. Oates AJ, Barraclough R, Rudland PS. The identification of osteopontin as a metastasis-related gene product in a rodent mammary tumour model. Oncogene 1996;13: 97–104.
31. Zhang S, Wang G, Liu D, et al. The C-terminal region of S100A4 is important for its metastasis-inducing properties. Oncogene 2005;24:4401–11.
32. Liu D, Rudland PS, Sibson DR, Platt-Higgins A, Barraclough R. Human homologue of cement gland protein, a novel metastasis inducer associated with breast carcinomas. Cancer Res 2005;65:3796–805.
33. Kerbel RS, Waghorne C, Man MS, Elliott B, Breitman ML. Alteration of the tumorigenic and metastatic properties of neoplastic cells is associated with the process of calcium phosphate-mediated DNA transfection. Proc Natl Acad Sci U S A 1987;84:1263–7.
34. Bertram J, Palfner K, Hiddemann W, Kneba M. Elevated expression of S100P, CAPL and MAGE 3 in doxorubicin-resistant cell lines: comparison of mRNA differential display reverse transcription-polymerase chain reaction and subtractive suppressive hybridization for the analysis of differential gene expression. Anticancer Drugs 1998;9:311–7.
35. Lloyd BH, Platt-Higgins A, Rudland PS, Barraclough R. Human S100A4 (p9Ka) induces the metastatic phenotype on benign tumour cells. Oncogene 1998;17: 465–73.
36. Mueller A, Bachi T, Hochli M, Schäfer BW, Heizmann CW. Subcellular distribution of S100 proteins in tumor cells and their relocation in response to calcium activation. Histochem Cell Biol 1999;111: 453–9.
37. Mandinova A, Atar D, Schäfer BW, Spiess M, Aebi U, Heizmann CW. Distinct subcellular localization of calcium binding S100 proteins in human smooth muscle cells and their relocation in response to rises in intracellular calcium. J Cell Sci 1998;111:2043–54.
38. Sorci G, Bianchi R, Giambanco I, Rambotti MG, Donato R. Replicating myoblasts and fused myotubes express the calcium-regulated proteins S100A1 and S100B. Cell Calcium 1999;25:93–106.
39. Rudland PS, Platt-Higgins AM, Wilkinson MC, Fernig DG. Immunocytochemical identification of basic fibroblast growth factor in the developing rat mammary gland: variations in location are dependent on glandular structure and differentiation. J Histochem Cytochem 1993;41:887–98.
40. Ambartsumian N, Klingelhofer J, Grigorian M, et al. The metastasis-associated Mts1(S100A4) protein could act as an angiogenic factor. Oncogene 2001;20: 4685–95.
41. Schmidt-Hansen B, Klingelhofer J, Grum-Schwensen B, et al. Functional significance of metastasis-inducing S100A4(Mts1) in tumor-stroma interplay. J Biol Chem 2004;279:24498–504.
42. van de Vijver MJ, He YD, van't Veer LJ, et al. A gene-expression signature as a predictor of survival in breast cancer. N Engl J Med 2002;347:1999–2009.
43. Vallely KM, Rustandi RR, Ellis KC, Varlamova O, Bresnick AR, Weber DJ. Solution structure of human Mts1 (S100A4) as determined by NMR spectroscopy. Biochemistry 2002;41:12670–80.